6.2

EXTRATROPICAL AIR-SEA INTERACTION DURING ENSO: ATMOSPHERIC FORCING AND OCEANIC FEEDBACKS

Michael Alexander and James Scott
NOAA-CIRES – Climate Diagnostics Center, Boulder, Colorado

Ileana Blade
LIM. Universitat Politècnica de Catalunya, Barcelona Spain

Clara Deser
NCAR, Boulder, Colorado

Gabriel Lau
GFDL/NOAA, Princeton, New Jersey

1. INTRODUCTION

Atmospheric teleconnections associated with ENSO alter the air temperature, humidity, wind, and clouds, which influence atmosphere-ocean interaction far from the equatorial Pacific. Thus, the atmosphere acts as a bridge from the ENSO region to the rest of the world's oceans, inducing changes in sea surface temperature (SST), salinity, mixed layer depth and ocean currents. The remote SST anomalies have the potential to feed back on the original atmospheric response to ENSO. Here, we examine the atmospheric bridge using 50 years of data (1950-1999) from the National Center for Environmental Prediction (NCEP) reanalysis project and a recently completed set of atmosphere-ocean model experiments.

2. MODEL SIMULATIONS

Most previous atmosphere-ocean modeling studies of the atmospheric bridge used coarse resolution (R15) atmospheric general circulation models (AGCMs), were based on a limited number of integrations (ensemble size < 5), and used different specified SST/ocean model configurations. To address these issues we have performed 32 new integrations with the GFDL R30 AGCM where all of

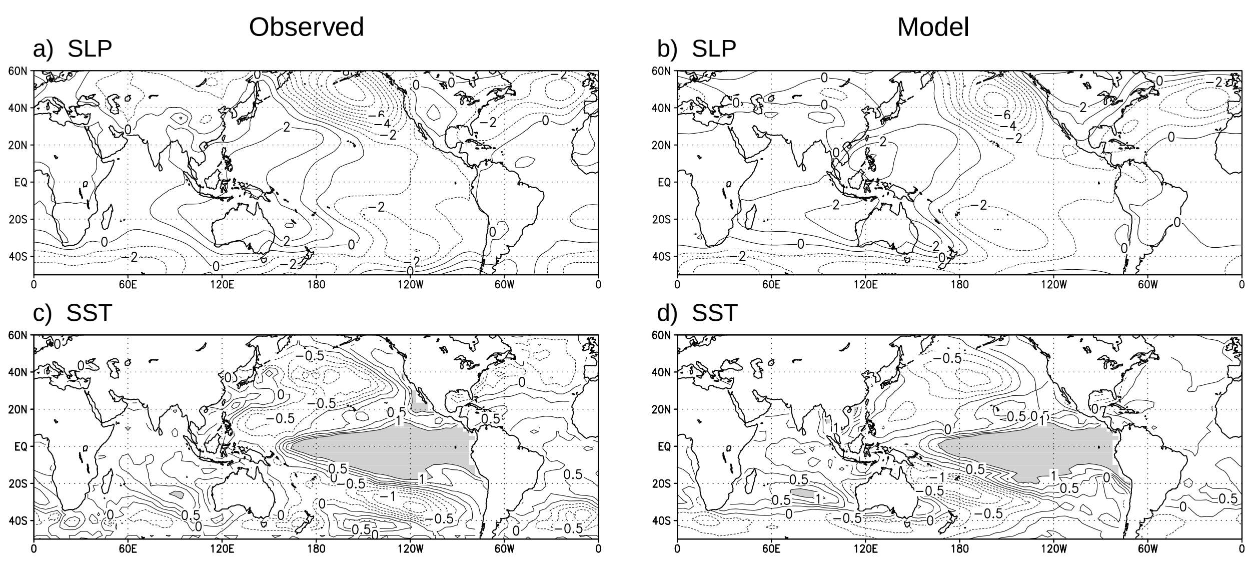

Fig. 1. El Niño (warm) – La Niña (cold) composite of a) Observed SLP, b) Simulated SLP (contour interval of 1 mb) and c) Observed SST, d) Simulated SST(contour interval of 0.25 ˚C for SST<1 ˚C; SST>1 ˚C shaded) during December-February , the "mature phase of ENSO". The observed values are from NCEP reanalysis and the model results from the ensemble average of the 16 MLM integrations.

the simulations have observed SSTs specified in the eastern tropical Pacific (15˚S-15˚N, 172˚E-South American Coast) over the period 1950-1999. Three sets of experiments have been conducted with different treatments of the ocean outside of this region. In the "**Control**" experiment, climatological SSTs, which repeat the same seasonal cycle each year, were specified at all remaining ocean grid points. In the mixed layer model ("**MLM**") experiment, a one-dimensional ocean model was coupled to the atmosphere at each ocean grid point outside of the tropical Pacific region. In the North Pacific – mixed layer model ("**NP-MLM"**) experiment, the ocean model is only active in the Pacific north of 21˚N; climatological SSTs were specified elsewhere over the global oceans. There are 8 Control, 8 NP-MLM and 16 MLM simulations.

3. RESULTS

Composites are constructed based on 9 El Niño (warm) and 9 La Niña (cold) events. Anomalies, defined here as the difference between the El

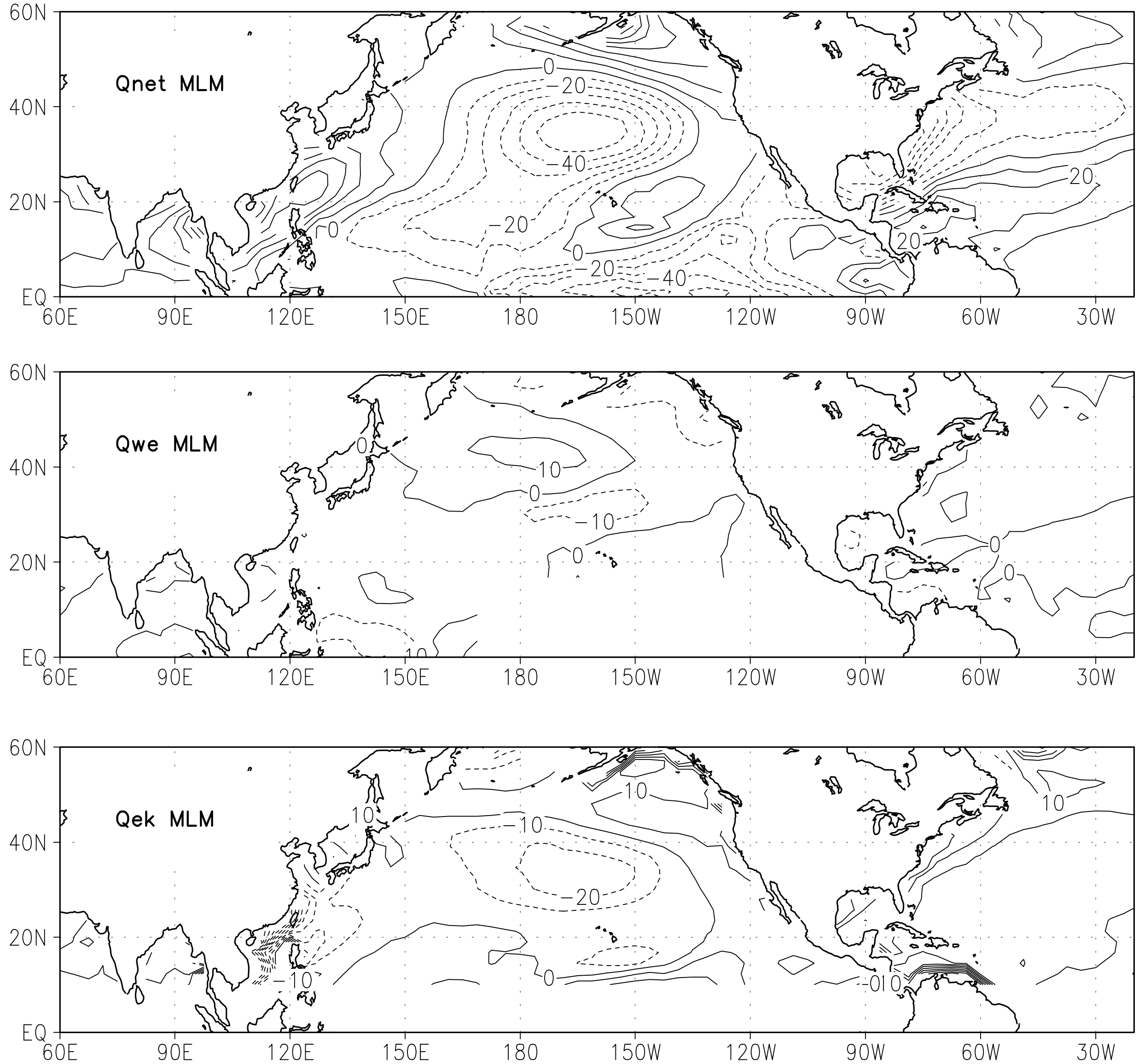

Fig. 2. The composite El Niño – La Niña a) net heat flux to the ocean (Q_{net}) b) entrainment heat flux (Q_{we}), and c) Ekman heat transport (Q_{ek}) during DJF from the MLM. The contour interval is 10 W m^{-2}.

Niño and La Niña composites are presented in Fig. 1 for SST and SLP during are December-January-February (DJF). Clearly, ENSO influences both the atmosphere and ocean over the entire globe. Cold SST anomalies (El Niño – La Niña) are found in the central North and South Pacific with warm SSTs along the west coast of North and South America. The Aleutian low is 9 (7) mb deeper in the observations (MLM) during El Niño compared with La Niña events. Assuming the winds are close to geostrophic balance, the surface westerlies are enhanced over the central North Pacific. In addition, anomalous northwest winds advect cold air over the central North Pacific, while southerly winds advect warm moist air along the west coast of North America during El Niño. Thus, the negative (positive) temperature departures in the central (eastern) North Pacific are consistent with the atmospheric circulation.

The MLM ensemble average warm-cold composite of the net surface heat flux into the ocean (Q_{net}), the entrainment heat flux at the base of the mixed layer (Q_{we}), and the Ekman heat transport (Q_{ek}) during DJF are shown in Fig. 2. Clearly, Q_{net} is the dominant term in creating SST anomalies during boreal winter. The maximum Q_{we} anomalies are roughly 1/4-1/3 as large as those of Q_{net} but have a different pattern, while the Ekman heat transport is generally in phase with Q_{net} but approximately 1/3-1/2 as large. The enhanced westerlies which increase upward surface heat flux during El Niño also create southward Ekman drift that cools the water in the central North Pacific.

Regression between the DJF ENSO index and MLD anomalies in JFM over the North Pacific are shown for observations and the MLM in Fig. 3. The observed MLD from White (1995) is estimated to be the depth at which the temperature is less than 1.0 ˚C cooler than the SST and is based on bathythermograph measurements for the years 1956-1995. The MLD is computed explicitly in the MLM based on the turbulent kinetic energy equation. The pattern of the ENSO-related MLD anomalies is similar in the observations and the model, with positive anomalies, indicating deeper mixed layers, in the center of the basin and negative anomalies in the northeast Pacific and to the south and east of Japan. Hanawa (1988) also noted shoaling of the mixed layer south of Japan during El Niño events. The pattern also resembles the ENSO SST anomaly pattern shown in Fig. 1, but with opposite polarity. The magnitude of the simulated and observed anomalies is comparable over most of the domain although the ENSO-related shoaling of the mixed layer west of Canada is weaker in the MLM. While many factors are likely to contribute to the model-data differences in the MLD, a potentially critical difference is that salinity is included in the ocean model but not in the observed MLD estimates. Salinity influences the-density profile and hence the base of the mixed layer, especially north of ~45 ˚N.

The extratropical height anomalies associated with ENSO take the familiar form of a wavetrain in the PNA region and are very similar in all three experiments, peaking in Jan-Feb and decaying thereafter. During Jan-Feb the anomalies are slightly weaker in the MLM and NP-MLM than in the control experiment, suggesting that coupling damps the mid winter response to ENSO (not shown but consistent with Alexander 1992, Blade 1997 and Newman et al. 2000). However, the most striking difference between the experiments occurs in March (Fig. 4) when the 500 mb height anomalies in the NP-MLM are substantially stronger than those in the Control. A similar but less conspicuous effect is found in the MLM experiment. The Control simulations underestimate the observed anomalies in March (Fig. 4d), the latter are more like the MLM (NP-MLM) over the North Pacific (Canada).

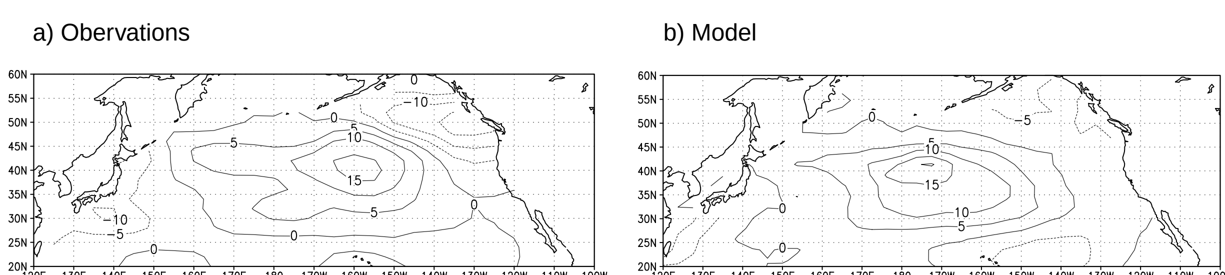

Fig 3. JFM Mixed Layer Depth (m) regressed with DJF ENSO index for a) 1956-1996 observations, b) 1950-1999 MLM.

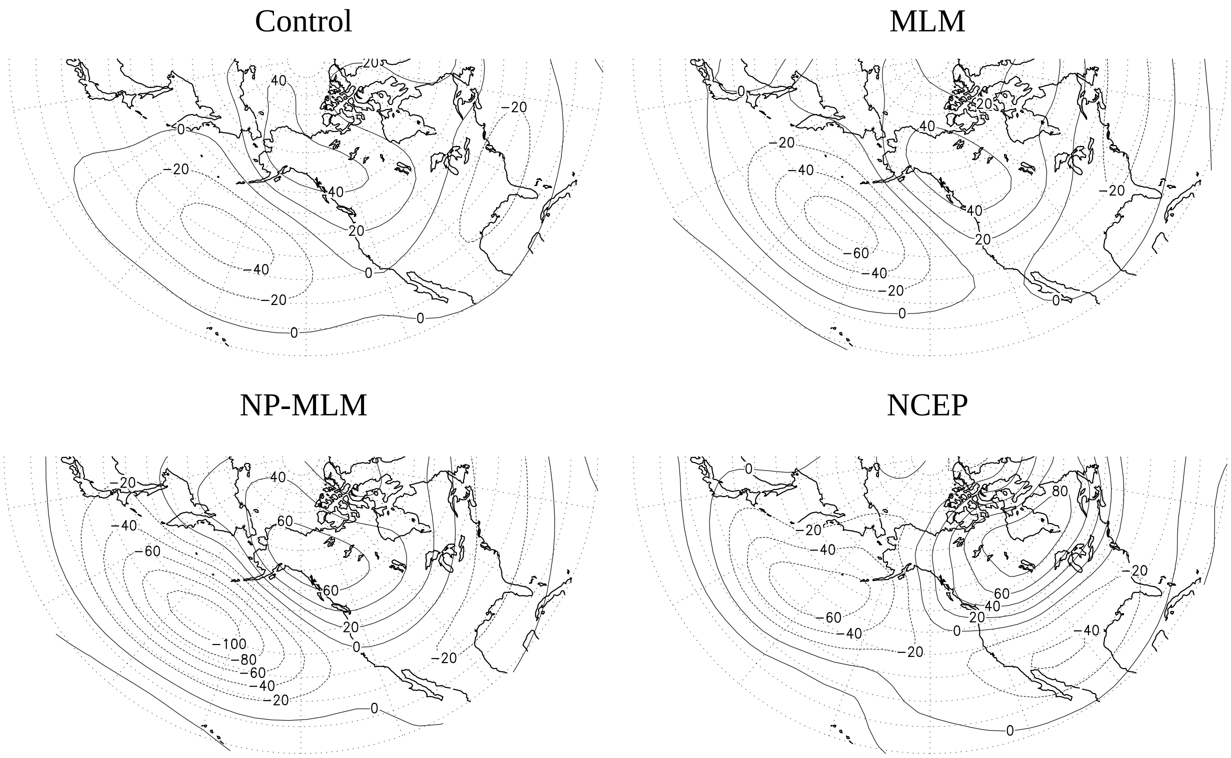

Fig. 4. The composite El Niño – La Niña 500 mb height from the a) Control, b) MLM, C) NP-MLM experiments and d) NCEP reanalysis during March. The contour interval is 20 m.

Our working hypothesis is that air-sea coupling in the North Pacific acts to enhance the atmospheric anomalies in the PNA region during March due to “reduced thermal damping” (Barsugli and Battisti 1997) and/or dynamical changes in the atmosphere, e.g. changes in storm tracks in response to anomalies in the local SST gradient. Differences between the NP-MLM and MLM 500 mb height anomalies could result from ENSO-related SST anomalies other regions influencing the atmosphere over the Northern Hemisphere. Preliminary results suggest that SST anomalies in the Indian Ocean in the MLM experiment, tend to create a high over the North Pacific, counteracting the direct response to ENSO.

4. REFERENCES

Alexander, M. A. 1992: Midlatitude atmosphere-ocean interaction during El Niño. Part II: the Northern Hemisphere atmosphere. *J. Climate*, **5**, 959-972.

Barsugli, J. J. and D. S. Battisti 1998: The basic effects of atmosphere-ocean thermal coupling on midlatitude variability. *J. Atmos. Sci.*, **55**,477-493.

Blade, I. 1999: The influence of midlatitude ocean-atmosphere coupling on the low-frequency variability of a GCM. Part II: Interannual variability induced by tropical SST forcing. *J. Climate*, **12**,21-45.

Newman, M., M. A. Alexander, C. R. Winkler, J. D. Scott, and J. J. Barsugli 2000: A linear diagnosis of the coupled extratropical Ocean-Atmosphere system in the GFDL GCM. *Atmospheric Sciences Letters*, **1**.